Central European Journal of Energetic Materials
ISSN 1733-7178; e-ISSN 2353-1843

Cent. Eur. J. Energ. Mater. 2026, *23*(1): 58-85; DOI 10.22211/cejem/220092
Article is available in PDF-format, in colour, at:
https://ipo.lukasiewicz.gov.pl/wydawnictwa/cejem-woluminy/vol-23-nr-1/

Research paper

Preparation and Properties of Melt-Cast Explosives Based on the Molecular Perovskite DAP-4

Xi Zhang[1)], **Li Yan**[2)], **Binfeng Sun**[3)], **Yibing Duan**[1)], **Yu Qiu**[1)], **Xiaoyu Shang**[1)], **Fuxing Wang**[1)], **Yang Liu**[1)], **Li-shuang Hu**[1,*)]

[1)] *School of Environment and Safety Engineering, North University of China, China*

[2)] *Houma Special Machinery Factory, China*

[3)] *Explosive Engineering and Safety Technology Research Institute of Ordnance Industry, China*

* *E-mail:* hlsly1314@163.com

Abstract: To reduce the high sensitivity of the molecular perovskite energetic material DAP-4 and enhance its practical utility, this study employed TNT and DNTF as melt-casting carriers to prepare DAP-4-based composite explosives. The morphology, thermal decomposition behavior, sensitivity, and detonation velocity of the composites were systematically investigated. Scanning electron microscopy observations showed that DAP-4 crystals retained their structural integrity and were uniformly coated by the carrier matrix. Differential scanning calorimetry analysis revealed that TNT delayed the high-temperature decomposition peak by up to 12.3 °C, whereas DNTF advanced it by up to 48.3 °C, indicating a catalytic effect. As the carrier content increased, the impact sensitivities of DAP-4/TNT and DAP-4/DNTF melt-cast explosives decreased from 100% to 16% and 40%, respectively, and both friction and electrostatic spark sensitivities were significantly reduced. Detonation velocity testing demonstrated that the DAP-4/TNT system exhibited increased velocity with higher DAP-4 content, while the velocities of DAP-4/DNTF systems are higher than that of the pure DAP-4, reaching a maximum detonation velocity of 8303 m/s. This study confirms that the melt-casting process can effectively balance energy output and safety, providing experimental support for the engineering application of DAP-4.

Keywords: melt-cast explosives, DAP-4, thermal decomposition, sensitivity reduction, detonation velocity

1 Introduction

In modern energetic materials, most practical explosives are multicomponent mixtures rather than single compounds. Among these, melt-cast explosives demonstrate superior comprehensive performance due to their molten-state processing capabilities. These systems not only conform to loading requirements for complex chamber geometries but also prove particularly valuable for military applications. Currently, melt-cast explosives are deployed worldwide for military purposes, constituting approximately 90% of military composite explosives by volume [1]. They represent core components of modern ordnance systems [2, 3]. Melt-cast explosives form a significant category of energetic materials. These systems are fabricated by uniformly dispersing solid-phase high explosives within molten liquid-phase carrier explosives, which are subsequently cooled and solidified to form multiphase composite energetic materials [4-6]. Among existing formulations, systems employing 2,4,6-trinitrotoluene (TNT) as the carrier, blended with high-energy-density compounds such as octahydro-1,3,5,7-tetranitro-1,3,5,7-tetrazocine (HMX) and cyclotrimethylenetrinitramine (RDX), represent the most common configurations. The classic Composition B explosive, comprising 40% TNT and 60% RDX by mass, is prepared through high-temperature fusion [7-11]. This composition achieves an optimal balance between detonation performance and processability. TNT exhibits a detonation velocity of 6970 m/s, detonation heat of 4148 kJ/kg, and a melting point of 80.9 °C. Its relatively low melting point and moderate detonation performance establish TNT as an ideal carrier for melt-cast explosives [12]. TNT offers significant economic advantages, including readily available raw materials and low production costs. Thermodynamically, its melting point (80.9 °C) is substantially lower than its thermal decomposition onset temperature (~280 °C), ensuring both safety and feasibility during melt-casting processes. Moreover, TNT exhibits remarkable chemical stability, is non-corrosive behavior toward metallic and maintains compatibility when blended with various high-energy explosives. These characteristics enable the formation of stable composite systems with excellent long-term storage stability [13-16]. 3,4-Bis (3-nitrofurazan-4-yl) furoxan (DNTF) is a novel high-energy-density compound developed in recent years. Its molecular structure contains two rings-a furfuryl oxide ring and two nitro groups (Figure 1 provides the molecular structure of DNTF). DNTF exhibits outstanding comprehensive properties, including a crystal

density of 1.937 g/cm^3, detonation velocity of 9250 m/s, detonation heat of 6054 kJ/kg, and a melting point of 110 °C. These characteristics make DNTF a highly promising material for a wide range of explosive applications [17]. The melting point of DNTF indicates excellent process compatibility and high thermal stability under prolonged heating conditions, with only minimal volatile losses, making it a highly suitable carrier for melt-cast explosives [18]. Research shows that, due to its unique molecular structure and favorable thermodynamic properties, DNTF remains processable in the molten state during the preparation of cast explosives. Moreover, when combined with other high-energy components, it significantly enhances the energy output of the explosive mixture. This combination of properties offers a promising technical pathway for developing high-energy-density energetic materials [19]. Furthermore, DNTF synthesis is straightforward and low-risk, while demonstrating excellent stability and safety [20-23]. As a new generation of high-energy-density material, DNTF holds a prominent position in the field of energetic compounds and serves as a key raw material for developing high-performance explosives.

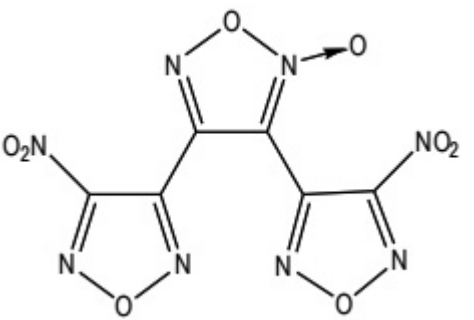

Figure 1. Molecular structures of DNTF

With ongoing advances in energetic materials research and technology, numerous novel energetic materials have been developed. Among these, molecular perovskite energetic materials have garnered significant research interest due to their distinctive crystal structures and superior properties. These materials demonstrate not only excellent detonation characteristics and high thermal stability but also offer considerable cost advantages. This class of ternary compounds employs low-cost organic fuels and oxidants components to form highly symmetrical perovskite structures (ABX_3) through close-packed stacking. In the crystal lattice, the A site is occupied by protonated organic cations that serve as fuels, including protonated triethylenediamine (H_2dabco^{2+}) and protonated piperazine (H_2pz^{2+}). The B site contains cations such as sodium (Na^+), potassium

(K^+), and ammonium (NH_4^+), while the X site is filled with strongly oxidizing anions, such as perchlorate (ClO_4^-) and nitrate (NO_3^-). A typical example is DAP-4 (chemical formula: $(H_2dabco)[NH_4(ClO_4)_3]$), a molecular perovskite energetic material with well-balanced properties that show great potential for applications in the field of energetic materials [24, 25]. Theoretical properties of DAP-4 include a crystal density of 1.87 g/cm^3, a detonation heat of 5.87 kJ/g, and a detonation pressure of 35.2 GPa, along with a measured detonation velocity of 8.806 km/s [26]. Current research indicates that DAP-4 possesses remarkable thermal stability [27-30], high output performance, low-cost raw materials, and a straightforward synthesis process. These advantages highlight its significant potential for energetic material applications and provide a valuable direction for developing novel energetic compounds [31-33]. The crystal density and theoretical detonation velocity of DAP-4 are comparable to those of RDX [26], while its thermal stability is significantly higher. However, its high sensitivity and low safety threshold considerably hinder its practical application [34, 35].

To address the high sensitivity of DAP-4, this study employed the formulation design principles of Explosive B, utilizing TNT and DNTF as castable carrier explosives. These were combined with the primary explosive, DAP-4, through a melt-casting process to produce a novel composite explosive exhibiting energy output and safety characteristics comparable to those of Explosive B. A systematic evaluation was conducted on key properties of the resulting composite, including morphology, thermal decomposition behavior, sensitivity parameters, and detonation velocity. This work aims to explore the application potential of DAP-4 in composite explosive systems and to provide both a theoretical foundation and experimental support for developing hybrid formulations with superior overall performance.

2 Experimental Section

2.1 Reagents and instruments

Reagents: TNT (Hubei Dongfang Chemical Co., Ltd.); DNTF (Gansu Yin'guang Chemical Industry Group Co., Ltd.); DAP-4 (prepared in the laboratory).

Instruments: TESCAN MIRA LMS Field Emission Scanning Electron Microscope (TESCAN Trading, Shanghai Co., Ltd.); Rigaku Miniflex 600 X-ray Diffractometer (Rigaku Corporation, Japan); DSC131 Differential Scanning Calorimeter (Setram Company); Impact Sensitivity Tester (IDEA SCIENCE Technology Corporation); Friction Sensitivity Tester (IDEA SCIENCE Technology Corporation); Electrostatic Spark Sensitivity Tester (IDEA SCIENCE

Technology Corporation); Detonation Velocity Tester (Hunan Xiangxi State Qibo Mining Instrument Factory).

2.2 Sample preparation

Based on the formulation design principles of Composition B explosive, DAP-4/TNT and DAP-4/DNTF melt-cast mixtures were prepared at mass ratios of 100:0, 50:50, 30:70, 10:90, and 0:100.

Preparation of explosive charges: Figure 2 illustrates the flowchart for sample preparation. Raw materials were weighed according to predetermined formulation ratios. TNT and DNTF were separately melted in glass beakers using an oven set to 100 and 150 °C, respectively. The molten liquids were then blended with gradually added DAP-4 under continuous stirring until homogeneous mixtures were formed. These mixtures were cast into preheated cylindrical Cr12MoV tool-steel molds with cavity dimensions of 10 mm in diameter and 10 mm in height. After demolding, the charges were machined to the target height and their bases were polished with abrasive paper. Final dimensions were verified using vernier calipers prior to detonation velocity testing. Figure 3 displays the DAP-4 explosives, Figure 4 shows the DAP-4/TNT melt-cast explosives, and Figure 5 presents the DNTF and DAP-4/DNTF melt-cast explosives, respectively. In order to eliminate the potential influence of the critical diameter on the detonation velocity of TNT, TNT charge samples measuring 40 mm in diameter and 32 mm in height were prepared, as shown in Figure 6.

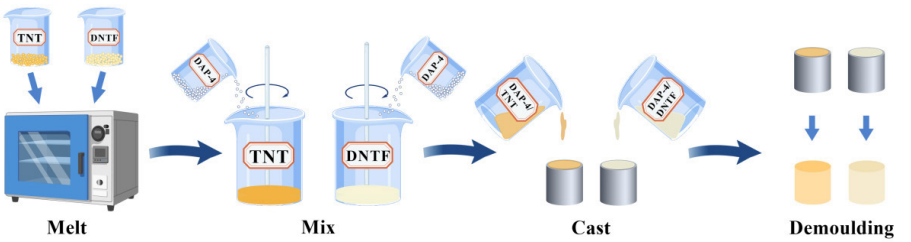

Figure 2. Schematic diagram of the sample preparation process

Figure 3. Photograph of DAP-4 charges

(a)

(b)

(c)

Figure 4. Photograph of DAP-4/TNT melt-cast charges: DAP-4:TNT=10:90 (a), DAP-4:TNT=30:70 (b) and DAP-4:TNT=50:50 (c)

(a)

(b)

(c)

(d)

Figure 5. Photograph of DNTF and DAP-4/DNTF melt-cast charges: DNTF (a), DAP-4:DNTF=10:90 (b), DAP-4:DNTF=30:70 (c) and DAP-4:DNTF=50:50 (d)

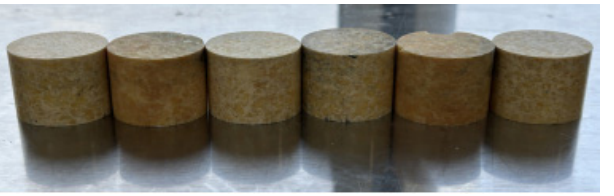

Figure 6. Photograph of TNT charges

Fabrication of powder samples: Procedures prior to mold casting followed the same protocol as explosive charge preparation. Once mixture homogeneity was achieved, the material was transferred to a sample tray and allowed to cool to room temperature under ambient conditions. The solidified sample was then pulverized using an agate mortar to produce, producing fine powder for subsequent differential scanning calorimetry (DSC) and sensitivity characterization of the melt-cast explosive.

The entire preparation procedure was carried out within an explosion-proof fume hood, following strict safety protocols to ensure operational safety. The total weight for a single batch of prepared samples does not exceed 10 g. For the grinding procedure, the amount of material processed per batch is limited to 50 mg or less.

2.3 Performance evaluation

Scanning electron microscopy (SEM) images of DAP-4, TNT, and DNTF raw materials, as well as prepared DAP-4/TNT and DAP-4/DNTF cast explosives, obtained using an acceleration voltage of 5 keV.

The crystalline structures of DAP-4, TNT, DNTF, and the prepared DAP-4/TNT and DAP-4/DNTF melt-cast explosives were analyzed using an X-ray diffractometer under the following conditions: a scanning angle range of 10° to 80°, a copper target, and a scanning speed of 2 °/min.

Differential Scanning Calorimetry (DSC) was employed to investigate the thermal decomposition properties of DAP-4, TNT, and DNTF raw materials, as well as the prepared DAP-4/TNT and DAP-4/DNTF melt-cast explosives. Sample weights were approximately 3 ±0.1 mg. A sealed aluminum crucible was used, with nitrogen as the protective gas at a flow rate of 50 mL/min. The heating rates were set at 5, 10, 15 and 20 °C/min, respectively. The testing temperature range was 30 to 600 °C.

Impact sensitivity of DAP-4, TNT, DNTF raw materials, and prepared DAP-4/TNT and DAP-4/DNTF melt-cast explosives was evaluated according to the GJB 772A-97 standard test methods for explosives. Testing parameters included a 1 kg drop hammer mass, a 200 mm drop height, and a 20 mg charge mass, with a total of 50 tests conducted in two sets of 25 trials each. Friction sensitivity was evaluated according to NATO Standard STANAG 4487 and MIL-STD-1751A: BAM Friction Test-Method 1024. Test parameters included a 5 ±1 mm^3 sample volume, with environmental conditions maintained at 20 ±5 °C and ≤80% relative humidity. Six tests were performed per experimental group.

Electrostatic spark sensitivity was evaluated according to Method 101 of the Chinese Military Standard GJB/Z 337A-94 (Langley Method). Testing was performed at 30 °C using an XSPARK-10 electrostatic sensitivity tester with supporting apparatus, and actual spark energy data were acquired via Win-Spark software. Each test series consisted of 30 shots.

The detonation velocities of the samples were measured in accordance with GJB 772A-97 Explosives Test Methods. Cylindrical charges measuring φ10×10 mm were used, with ignition initiated by 0.1 mm diameter enameled copper wire probes. The test consisted of two experimental groups, each with four replicate charges.

3 Results and Discussion

3.1 SEM Microstructure Characterization

The microstructural analysis of explosive samples enables direct visualization of changes in crystal surface morphology within composite materials. To achieve this, SEM was employed to characterize the microstructure of DAP-4, TNT, DNTF, and their composites DAP-4/TNT and DAP-4/DNTF at varying mass ratios. These results are presented in Figure 7. As shown in Figure 7(a), DAP-4 crystals exhibit a regular cubic shape with sharp edges and smooth surfaces. Figure 7(b) reveals that TNT displays an irregular block-like structure with a relatively rough surface and prominent edges. Meanwhile, DNTF in Figure 7(c) shows an irregular block-like structure with uneven surfaces and numerous edges. Figures 7(d-f) show that in the DAP-4/TNT melt-casting system, DAP-4 crystals retain their original discrete structure, while molten TNT disperses around these crystals. As the TNT mass fraction increases, the encapsulation of DAP-4 crystals by TNT becomes more extensive. Notably, the two components form intimate interfacial contact, demonstrating good homogeneity within the blended system. Figures 7(g-i) demonstrate that in the DAP-4/DNTF melt-casting system, DAP-4 crystals preserve their discrete structure. Molten DNTF is uniformly dispersed among and around these crystals. With increasing DNTF content, a greater proportion of DNTF accumulates and adheres to the DAP-4 crystal surfaces. The images confirm tight interfacial bonding between the components, verifying effective mixing and mixture homogeneity.

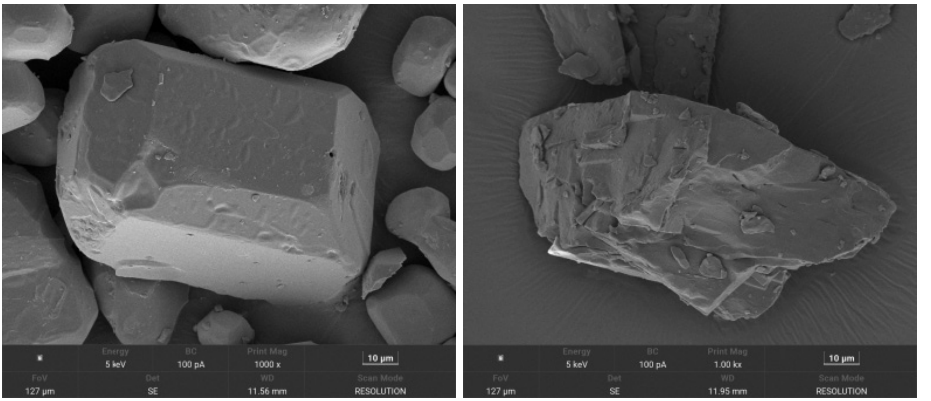

(a) (b)

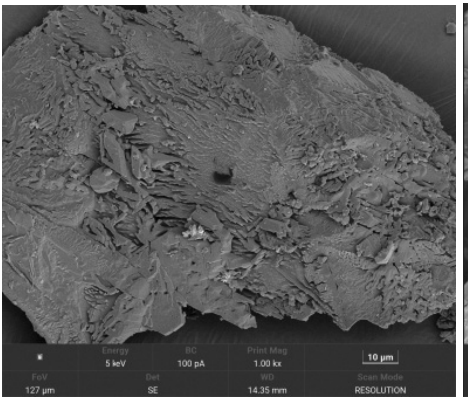

(c)

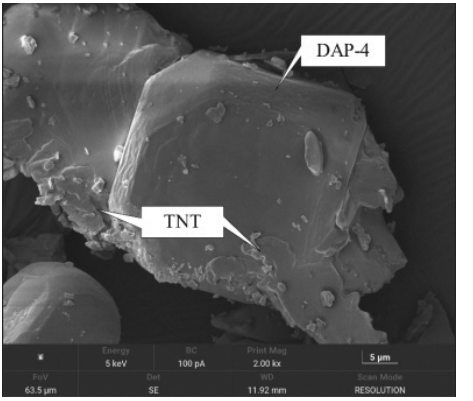

(d)

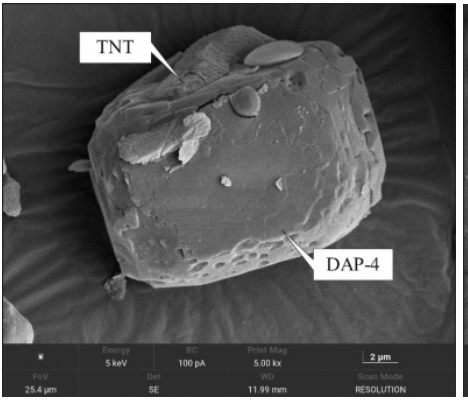

(e)

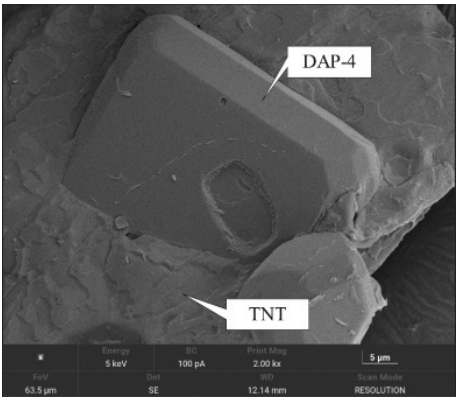

(f)

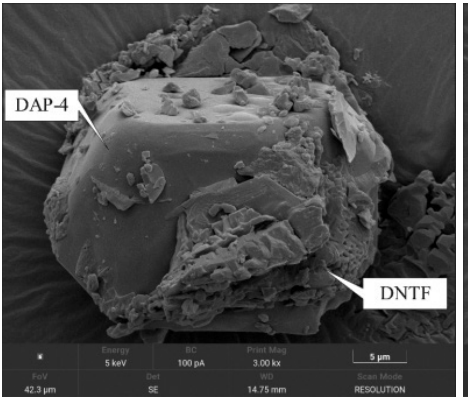

(g)

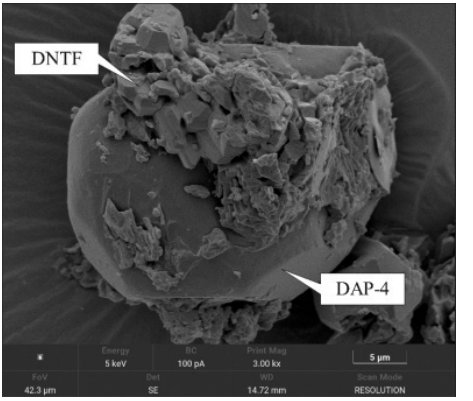

(h)

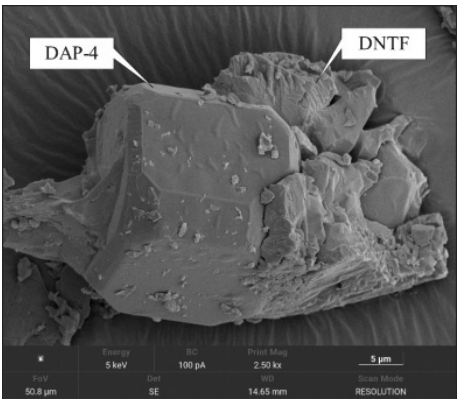

(i)

Figure 7. SEM images of DAP-4, TNT, DNTF, and DAP-4/TNT and DAP-4/DNTF melt-cast explosives with different mass ratios: DAP-4 (a), TNT (b), DNTF (c), DAP-4:TNT=50:50 (d), DAP-4:TNT=30:70 (e), DAP-4:TNT=10:90 (f), DAP-4:DNTF=50:50 (g), DAP-4:DNTF=30:70 (h) and DAP-4:DNTF=10:90 (i)

3.2 XRD characterization

The crystalline structures of DAP-4, TNT, DNTF, and the prepared DAP-4/TNT and DAP-4/DNTF melt-cast explosives with varying ratios were characterized by X-ray diffraction (XRD). The resulting XRD patterns are presented in Figure 8. As shown in Figure 8(a), DAP-4/TNT melt-cast explosives with different ratios display a consistent set of diffraction peaks, notably at 2θ values of 12.24°, 12.62°, 17.76°, 21.21°, 22.97°, 24.55°, 27.48°, 29.27°, 33.51°, 36.60°, and 37.15°. This set of peaks corresponds to a simple superposition of the characteristic peaks from the individual DAP-4 and TNT crystals, with only the relative intensities varying across the different melt-cast explosive systems. A similar phenomenon is observed for the DAP-4/DNTF melt-cast explosive system in Figure 8(b), where peaks appear at 2θ = 11.75°, 12.24°, 16.58°, 21.13°, 21.21°, 23.52°, 24.55°, 27.48°, 28.21°, 33.44°, 36.60°, and 37.15°. Again, the pattern essentially represents a superposition of the monomer peaks, with relative intensities varying as a function of the compositional ratio in these melt-cast explosive systems. The experimental XRD pattern of as-prepared DAP-4 shows peaks at 12.24°, 21.21°, 24.55°, 27.48°, 36.60°, and 37.15°. These peak positions match the simulated pattern from the single-crystal structure (CCDC: 152810), corresponding to the (200), (222), (400), (420), (531), and (600) crystal planes, respectively. This agreement confirms that the synthesized sample is phase-pure DAP-4. Further analysis indicates that the crystal structure of DAP-4 remains unaltered by

TNT or DNTF during the melting process, suggesting that the fusion is a purely physical mixture without chemical reaction. This effectively preserves the intrinsic properties of DAP-4. The observed differences in relative diffraction peak intensities between the two cast explosives can be attributed to the adherence of TNT or DNTF crystalline particles onto the surfaces of DAP-4 crystals. This surface coverage likely obscures the diffraction signals from specific crystal planes of DAP-4, thereby reducing the intensities of the corresponding peaks.

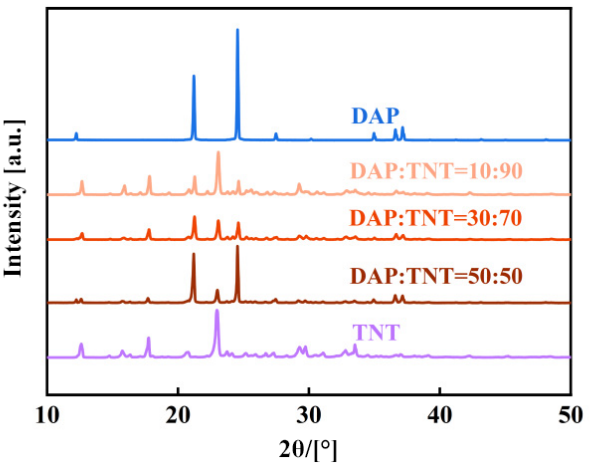

(a)

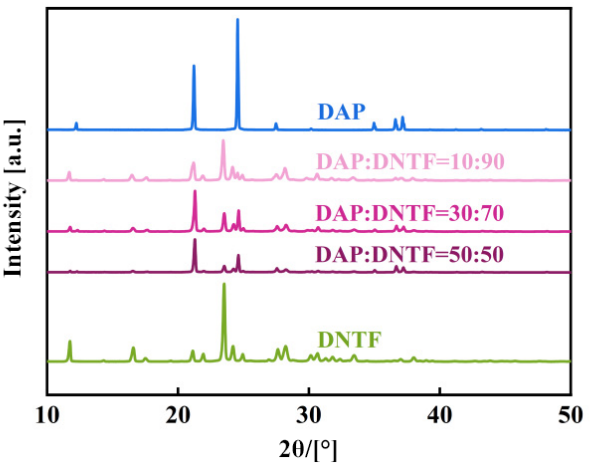

(b)

Figure 8. XRD patterns of DAP-4, TNT, DNTF, and their melt-cast explosives with varying DAP-4/TNT (a) and DAP-4/DNTF (b) ratios

3.3 DSC characterization

To assess the thermal stability of cast explosives, differential scanning calorimetry (DSC) was employed to characterize their thermal decomposition behavior. Figures 9 and 10 present the DSC curves measured at different heating rates for the DAP-4/TNT and DAP-4/DNTF systems, respectively. Specifically, Figure 9 includes the curves for DAP-4, TNT, and their melt-cast explosives, while Figure 10 shows the curves for DAP-4, DNTF, and their melt-cast explosives, each with varying mass ratios. The corresponding decomposition temperatures are summarized in Tables 1-5.

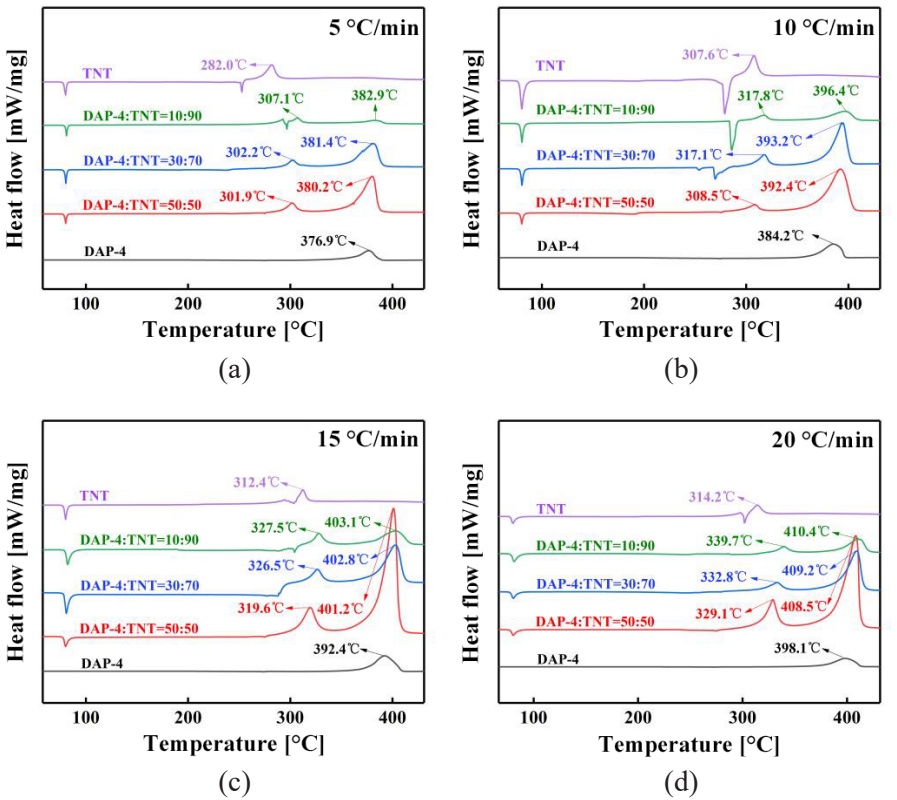

Figure 9. DSC curves of DAP-4, TNT and DAP-4/TNT melt-cast explosive samples with different mass ratios under different heating rates: 5 (a), 10 (b), 15 (c) and 20 °C/min (d)

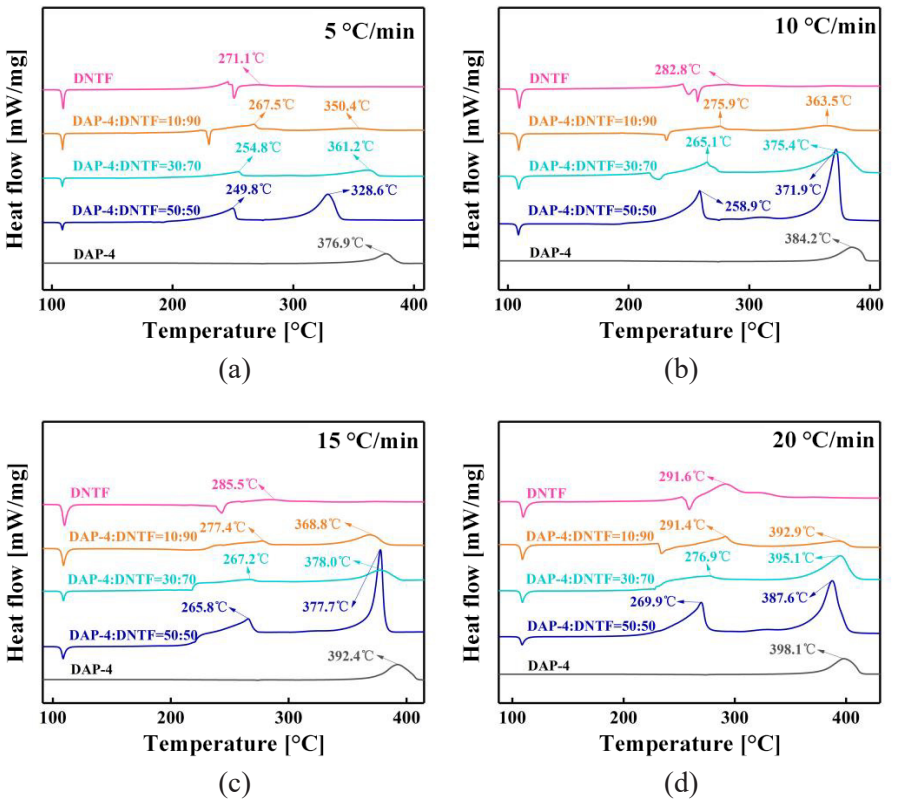

Figure 10. DSC curves of DAP-4, DNTF and DAP-4/DNTF melt-cast explosive samples with different mass ratios under different heating rates: 5 (a), 10 (b), 15 (c) and 20 °C/min (d)

Table 1. Decomposition temperatures of pure DAP-4, TNT and DNTF at varying heating rates

Sample	Decomposition peak temperature [°C] at varying heating rates (in °C/min)			
	5	10	15	20
DAP-4	376.9	384.2	392.4	398.1
TNT	282.0	307.6	312.4	314.2
DNTF	271.1	282.8	285.5	291.6

Table 2. Low-temperature decomposition peak temperatures of DAP-4/TNT melt-cast explosives with varying mass ratios at multiple heating rates

DAP-4:TNT	Low-temperature decomposition peak temperature [°C] at varying heating rates (in °C/min)			
	5	10	15	20
50:50	301.9	308.5	319.6	329.1
30:70	302.2	317.1	326.5	332.8
10:90	307.1	317.8	327.5	339.7

Table 3. High-temperature decomposition peak temperatures of DAP-4/TNT melt-cast explosives with varying mass ratios at multiple heating rates

DAP-4:TNT	High-temperature decomposition peak temperature [°C] at varying heating rates (in °C/min)			
	5	10	15	20
50:50	380.2	392.4	401.2	408.5
30:70	381.4	393.2	402.8	409.2
10:90	382.9	396.4	403.1	410.4

Table 4. Low-temperature decomposition peak temperatures of DAP-4/DNTF melt-cast explosives with varying mass ratios at multiple heating rates

DAP-4:DNTF	Low-temperature decomposition peak temperature [°C] at varying heating rates (in °C/min)			
	5	10	15	20
50:50	249.8	258.9	265.8	269.9
30:70	254.8	265.1	267.2	276.9
10:90	267.5	275.9	277.4	291.4

Table 5. High-temperature decomposition peak temperatures of DAP-4/DNTF melt-cast explosives with varying mass ratios at multiple heating rates

DAP-4:DNTF	High-temperature decomposition peak temperature [°C] at varying heating rates (in °C/min)			
	5	10	15	20
50:50	328.6	371.9	377.7	387.6
30:70	362.1	375.4	378.0	395.1
10:90	350.4	363.5	368.8	392.9

3.3.1 DSC characterization of DAP-4/TNT melt-cast explosives

Analysis of the thermal decomposition behavior of pure DAP-4 and TNT, supported by data in Figure 9(a-d) and Table 1, reveals that DAP-4 displays an endothermic peak with a temperature that remains constant at 273.4 °C, independent of the heating rate. This corresponds to a reversible phase transition, as confirmed in prior studies [34]. At heating rates of 5 and 20 °C/min, decomposition peak temperatures are observed at 376.9 and 398.1 °C, respectively, demonstrating high thermal stability. TNT melts at 80.1 °C, accompanied by an endothermic peak. When heated at 5 °C/min, its exothermic decomposition occurs at 282.0 °C. Increasing the heating rate to 20 °C/min raises the decomposition temperature to 314.2 °C, consistent with kinetic relaxation principles.

Analysis of the thermal decomposition behavior of DAP-4/TNT cast explosives, as shown in Figure 9(a-d), reveals a biphasic decomposition process corresponding to the characteristic decomposition peak temperatures of TNT and DAP-4. The lower-temperature phase, associated with TNT decomposition, is summarized in Table 2, while the higher-temperature phase, related to DAP-4 decomposition, is provided in Table 3. The first endothermic peak at 80.1 °C corresponds to the melting of TNT, consistent with the endothermic behavior of pure TNT. The second endothermic peak at 273.4 °C corresponds to the phase transition of DAP-4. At a heating rate of 5 °C/min, the high-temperature decomposition peaks for DAP-4: TNT mixtures with ratios of 50:50, 30:70, and 10:90 occur at 380.2, 381.4 and 382.9 °C, respectively. Compared to pure DAP-4, all samples exhibit a delay in decomposition temperature ranging from 3.3 to 6.0 °C at this heating rate. At a heating rate of 10 °C/min, the high-temperature decomposition peaks for the same mixtures occur at 392.4, 393.2 and 396.4 °C, respectively, showing a delay of 8.2 to 12.2 °C relative to pure DAP-4. At a heating rate of 15 °C/min, the peaks occur at 401.2, 402.8 and 403.1 °C, respectively, with a delay ranging from 8.8 to 10.7 °C compared to pure DAP-4. At a heating rate of 20 °C/min, the peaks occur at 408.5, 409.2 and 410.4 °C, respectively, exhibiting a delay of 10.4 to 12.3 °C relative to pure DAP-4. Under constant heating rates, the high-temperature decomposition peaks of DAP-4/TNT melt-cast mixtures systematically shift to higher temperatures with increasing TNT content compared to pure DAP-4. At all tested heating rates, the decomposition peak temperatures of the composite mixtures are significantly delayed relative to pure DAP-4. This demonstrates that incorporating TNT substantially enhances the thermal stability of the DAP-4/TNT melt-cast system.

3.3.2 DSC characterization of DAP-4/DNTF melt-cast explosives

Analysis of the thermal decomposition behavior of pure DAP-4 and DNTF, supported by data in Figure 10(a-d) and Table 1, reveals that the thermal decomposition behavior of DAP-4 is consistent with the analysis presented in section 3.3.1. DNTF melts at 109.4 °C, also with an endothermic peak. At a heating rate of 5 °C/min, decomposition occurs at 271.1 °C. When the heating rate increases to 20 °C/min, the peak temperature rises to 291.6 °C, indicating comparatively low sensitivity to heating rate variations.

As shown in Figure 10(a-d), the two-stage decomposition behavior of DAP-4/DNTF cast explosives is quantified in Tables 4 and 5. Specifically, Table 4 lists the peak temperatures for the low-temperature stage, and Table 5 provides those for the high-temperature stage. This behavior corresponds to the distinct decomposition peak temperatures of DNTF and DAP-4. The initial endothermic peak occurs at 109.4 °C, corresponding to the melting transition observed in pure DNTF. A subsequent endothermic peak appears at 273.4 °C, consistent with the phase transition temperature of DAP-4. At a heating rate of 5 °C/min, the high-temperature decomposition peaks for DAP-4:DNTF mixtures with ratios of 50:50, 30:70, and 10:90 occur at 328.6, 362.1 and 350.4 °C, respectively. Compared to pure DAP-4, all mixtures exhibit decomposition temperatures that occur 15.7 to 48.3 °C earlier at this heating rate. At a heating rate of 10 °C/min, the corresponding peaks occur at 371.9, 375.4 and 363.5 °C, respectively, representing 8.8 to 20.7 °C earlier decomposition than pure DAP-4. At a heating rate of 15 °C/min, the peaks occur at 377.7, 378.0 and 368.8 °C, respectively, which is 14.4 to 23.6 °C earlier than pure DAP-4. At a heating rate of 20 °C/min, the peaks occur at 387.6, 395.1 and 392.9 °C, respectively, showing a 3.0 to 10.5 °C earlier decomposition compared to pure DAP-4. Under constant heating rates, the high-temperature decomposition peaks of DAP-4/DNTF melt-cast mixtures systematically shift to lower temperatures with increasing DNTF content, thereby advancing the decomposition process. The high-temperature decomposition peak temperatures of all composite systems are significantly lower than those of pure DAP-4 under the same heating conditions. This systematic advancement indicates that the decomposition products of DNTF have a catalytic effect on the pyrolysis process of DAP-4.

3.4 Assessment of sensitivity and explosive performance

The results of impact sensitivity, friction sensitivity, and electrostatic spark sensitivity tests for DAP-4, TNT, DNTF, and DAP-4/TNT and DAP-4/DNTF cast explosives with varying mass ratios are shown in Table 6. As shown, DAP-4 exhibits high sensitivity, with 100% impact sensitivity, 40 N friction

sensitivity, and 128.39 mJ electrostatic spark sensitivity. Both TNT and DNTF demonstrate 0% impact sensitivity and 360 N friction sensitivity. Additionally, TNT has an electrostatic spark sensitivity of 1063.20 mJ, while DNTF measures 1019.30 mJ, both indicating excellent insensitivity characteristics. The cast explosive with a DAP-4:TNT mass ratio of 50:50 exhibited an impact sensitivity of 60%, a friction sensitivity of 160 N, and an electrostatic spark sensitivity of 418.15 mJ. At the 30:70 DAP-4:TNT ratio, the impact sensitivity was 40%, friction sensitivity 360 N, and electrostatic spark sensitivity 555.40 mJ. The 10:90 DAP-4:TNT formulation showed an impact sensitivity of 16%, a friction sensitivity of 360 N, and an electrostatic spark sensitivity of 818.54 mJ. For DAP-4:DNTF compositions, the 50:50 mass ratio explosive exhibited an impact sensitivity of 80%, a friction sensitivity of 80 N, and an electrostatic spark sensitivity of 444.90 mJ. The 30:70 DAP-4:DNTF blend exhibited an impact sensitivity of 57%, a friction sensitivity of 120 N, and an electrostatic spark sensitivity of 538.15 mJ. The 10:90 DAP-4:DNTF composition exhibited an impact sensitivity of 40%, a friction sensitivity of 240 N, and an electrostatic spark sensitivity of 781.89 mJ.

Table 6. Sensitivity characterization of DAP-4, TNT, DNTF, DAP-4/TNT, and DAP-4/DNTF melt-cast explosives at varying mass ratios

Sample	Impact sensitivity [%]	Friction sensitivity [N]	Electrostatic spark sensitivity [mJ]
DAP-4	100	40	128.39
TNT	0	360	1063.20
DNTF	0	360	1019.30
DAP-4:TNT			
– 50:50	60	160	418.15
– 30:70	40	360	555.40
– 10:90	16	360	818.54
DAP-4:DNTF			
– 50:50	80	80	444.90
– 30:70	57	120	538.15
– 10:90	40	240	781.89

Sensitivity testing of melt-cast DAP-4/TNT and DAP-4/DNTF formulations with varying mass ratios demonstrates that increasing the content of TNT or DNTF progressively reduces impact sensitivity. Concurrently, friction sensitivity decreases, as indicated by a gradual increase in the load required to initiate a reaction. Similarly, electrostatic spark sensitivity diminishes, evidenced by

an increase in the triggering energy. Overall, incorporation of TNT or DNTF effectively desensitizes DAP-4, significantly reducing both its mechanical and electrostatic spark sensitivities.

To evaluate the energetic contributions of DAP-4/TNT and DAP-4/DNTF formulations in composite explosive systems, we calculated the densities of DAP-4, TNT, DNTF, and their melt-cast blends at various mass ratios and measured the corresponding detonation velocities. The experimental setup and the corresponding post-test conditions are illustrated in Figures 11 and 12, respectively. Figure 11 shows a schematic of the blast velocity test setup, while Figure 12 presents photographs of the test base components after the experiment, including DAP-4, TNT, DNTF, and their melt-cast explosives with varying DAP-4/TNT and DAP-4/DNTF ratios. A comparative analysis is provided in Table 7. For each sample listed in Table 7, density was measured using eight replicates, and the results are presented as the mean value with the standard deviation (mean ±SD).

(a)

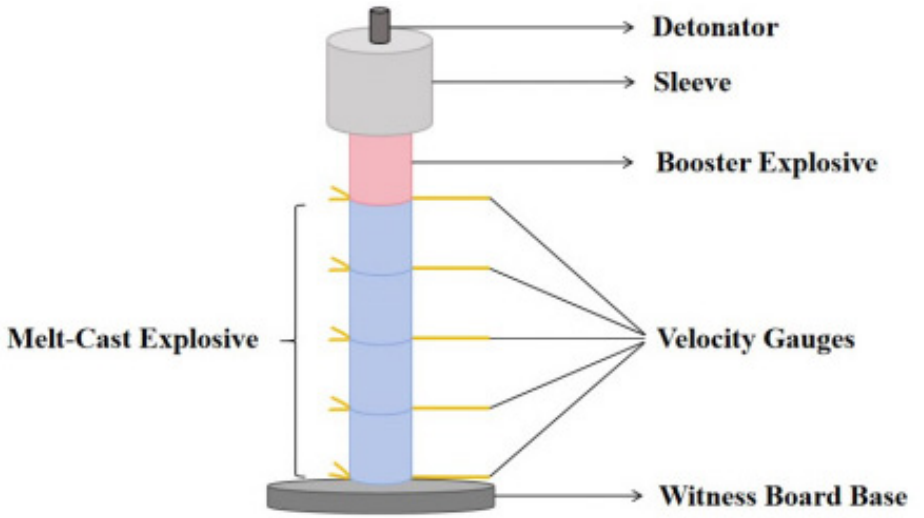

(b)

Figure 11. Schematic of the blast velocity test setup: pre-test photograph of a columnar sample (a) and the scheme of the detonation velocity test (b)

(a)

(b)

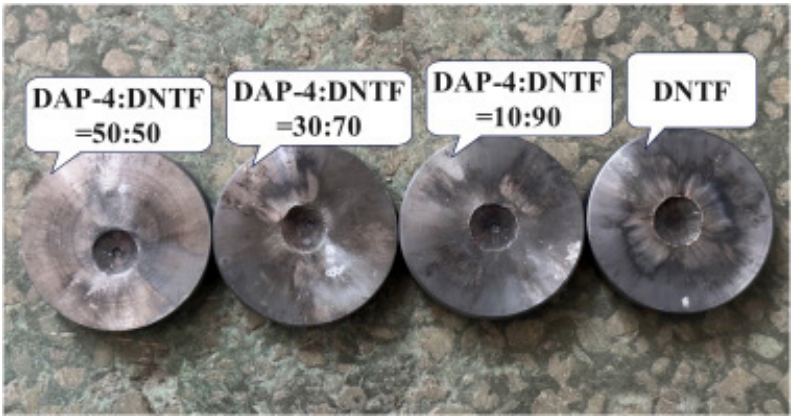

(c)

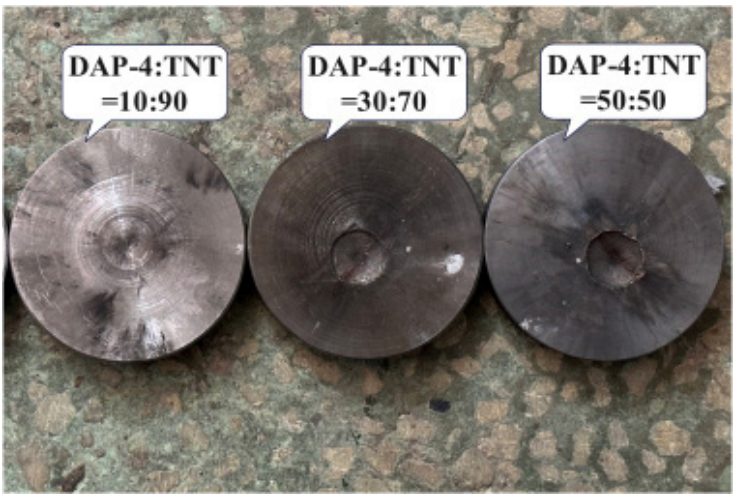

(d)

Figure 12. Photographs of the test base components after the experiment: TNT (a), DAP-4 (b), DNTF (c), and their melt-cast explosives with varying DAP-4/DNTF (c) and DAP-4/TNT (d) ratios

Table 7. Detonation velocity test results for DAP-4, TNT, DNTF, DAP-4/TNT, and DAP-4/DNTF melt-cast explosives with different mass ratios

Sample	DAP-4	TNT	DNTF	DAP-4:TNT			DAP-4:DNTF		
				50:50	30:70	10:90	50:50	30:70	10:90
Density [g/cm^3]	1.58 ±0.01	1.51 ±0.01	1.70 ±0.01	1.66 ±0.02	1.63 ±0.01	1.57 ±0.01	1.77 ±0.03	1.77 ±0.03	1.74 ±0.01
Detonation velocity [m/s]	7852	5056	8652	7488	6913	5579	8019	8292	8303

As shown in Table 7, the detonation velocity results represent the average of four independent measurements obtained using the detonation velocity meter. The DAP-4 propellant column was prepared using a compression molding process, achieving a density of 1.58 ±0.01 g/cm^3 and a measured detonation velocity of 7852 m/s. The TNT exhibited molded density of 1.51 ±0.01 g/cm^3 and a detonation velocity of 5056 m/s. The DNTF had a molded density of 1.70 ±0.01 g/cm^3 and a detonation velocity of 8652 m/s. The 50:50 DAP-4/TNT cast explosive formulation exhibited a molded density of 1.66 ±0.02 g/cm^3 and a detonation velocity of 7488 m/s, representing an 84.6% increase relative to TNT.

The 30:70 DAP-4/TNT formulation showed a density of 1.63 ±0.01 g/cm^3 with a detonation velocity of 6913 m/s, corresponding to a 70.4% enhancement over TNT. For the 10:90 DAP-4/TNT ratio, the molded density was 1.57 ±0.01 g/cm^3, and the detonation velocity reached 5579 m/s, reflecting a 37.5% improvement compared to TNT. In the DAP-4/TNT cast explosive system, detonation velocity increases substantially with rising DAP-4 mass fraction, demonstrating DAP-4's significant energetic contribution to the TNT-based formulation and effectively elevating the system's energy output. Consequently, DAP-4 markedly enhances the detonation performance of TNT-based cast explosives. The 50:50 DAP-4/DNTF cast explosive formulation exhibited a molded density of 1.77 ±0.03 g/cm^3 and a detonation velocity of 8019 m/s, representing a 2.1% increase over pure DAP-4. At the 30:70 DAP-4/DNTF ratio, the formulation maintained the same density of 1.77 ±0.03 g/cm^3 with a detonation velocity of 8292 m/s, corresponding to a 5.6% enhancement. The 10:90 formulation had a density of 1.74 ±0.01 g/cm^3 and achieved a detonation velocity of 8303 m/s, reflecting a 5.7% improvement relative to DAP-4. Due to DNTF's significantly higher detonation velocity compared to DAP-4, The detonation velocity of the DAP-4/DNTF cast explosive system decreases as the DAP-4 mass fraction increases. Nevertheless, all DAP-4/DNTF formulations exhibit detonation velocities exceeding that of pure DAP-4, demonstrating the overall superior detonation performance of the DNTF-based system.

Concerning safety performance, the DAP-4/TNT melt-cast system exhibits superior thermal stability and reduced mechanical sensitivity. The thermal decomposition temperature is significantly elevated, while sensitivity to mechanical stimuli is markedly decreased, indicating enhanced chemical stability and operational safety. These properties make it especially suitable for long-term storage, transportation under complex environmental conditions, and weapon propellants requiring high reliability.

Regarding energy output, the DAP-4/DNTF system capitalizes on the inherent high-energy characteristics of DNTF, achieving high detonation velocities and efficient energy release. This system is therefore better suited for applications where destructive power is critical, such as breaching warheads, explosive initiation trains, and specialized penetration missions. Furthermore, it extends the operational range of melt-cast explosives and allows for tunable energy output.

4 Conclusions

- DSC analysis revealed contrasting thermal behaviors in melt-cast systems. Increasing the TNT content in DAP-4/TNT composites delayed the high-temperature decomposition peak by up to 12.3 °C compared to pure DAP-4, indicating enhanced thermal stability. Conversely, higher DNTF content in DAP-4/DNTF composites advanced the peak temperature by 48.3 °C. This acceleration indicates catalytic activity of DNTF decomposition products on DAP-4 pyrolysis, which has implications for process safety controls.
- Based on a comprehensive evaluation of detonation velocity and sensitivity, both the DAP-4/TNT and DAP-4/DNTF composite systems demonstrate a well-balanced synergy between energy performance and safety. The DAP-4:TNT = 50:50 formulation achieved a detonation velocity of 7488 m/s, which is 84.6% higher than that of pure TNT, while showing significantly improved safety characteristics compared to pure DAP-4: impact sensitivity was reduced from 100% to 60%, friction sensitivity increased from 40 to 160 N, and electrostatic spark sensitivity rose from 128.39 to 418.15 mJ. Similarly, the DAP-4:DNTF = 10:90 system attained the highest detonation velocity of 8303 m/s, exceeding that of pure DAP-4, while demonstrating remarkable desensitization relative to pure DAP-4: impact sensitivity decreased to 40%, friction sensitivity increased to 240 N, and electrostatic spark sensitivity rose to 781.89 mJ.
- This study demonstrates that melt-casting with either TNT or DNTF effectively modulates the properties of DAP-4, achieving an optimal balance between energy content and safety. By demonstrating the practical utility of molecular perovskite energetic materials in melt-cast explosives, our work expands design strategies for high-energy, low-sensitivity formulations and provides key insights for their engineering applications.

Acknowledgments

This work was supported by the National Natural Science Foundation of China (No. 52276138).

References

[1] Kuang, B.; Wang, T.; Li, C.; Sun, M.; Tariq, Q.-un-N.; Zhang, C.; Xie, Z.M.; Lu, Z.J.; Zhan, J.G. Dinitrophenyl-oxadiazole Compounds: Design Strategy, Synthesis, and Properties of a Series of New Melt-Cast Explosives. *Def. Technol.* **2024**, *35*: 100-107; https://doi.org/10.1016/j.dt.2023.11.022.

[2] Zheng, B.H.; Luo, G.; Shu, Y.J. Research Status and Prospect of Melt-cast Explosive. *Chem. Ind. Eng. Prog.* **2013**, *32*(06): 1341-1346; https://doi.org/10.3969/j.issn.1000-6613.2013.06.023.

[3] Wang, X.F. Developmental Trends in Military Composite Explosive. *Chin. J. Explos. Propellants* **2011**, *34*(04): 1-4+9; https://doi.org/10.14077/j.issn.1007-7812.2011.04.019.

[4] Zhu, J.W.; Wang, L.J.; Liu, Y.C. Preparation and Properties of 2,4-MDNI/DNTF Binary Eutectic. *Chin. J. Energ. Mater.* **2022**, *30*(03): 228-235; https://doi.org/10.11943/CJEM2021166.

[5] Wang, S.W.; Zhang, Y.L.; Wu, C.; Xiao, L.; Lin, G.M.; Hu, Y.B..; Hao, G.Z.; Guo, H.; Zhang, G.P.; Jiang, W. Equal-Material Manufacturing of a Thermoplastic Melt-Cast Explosive Using Thermal-Pressure Coupling Solidification Treatment Technology. *ACS Omega* **2023**, *8*(18): 16251-16262; https://doi.org/10.1021/acsomega.3c00709.

[6] Reinhardt, E.; Lenz, T.; Bauer, L.; Stierstorfer, J.; Klapotke, T.M. Synthesis and Characterization of Azido-and Nitratoalkyl Nitropyrazoles as Potential Melt-Cast Explosives. *Molecules* **2023**, *28*(18): 6489; https://doi.org/10.3390/molecules28186489.

[7] Li, M.; Cheng, Y.F.; Wang, R.; Wang, Q.; Mogi, T. Study on the Mutual Feedback Effects in Gas-Solid Two-Phase Combustion of TiH_2 Dust Clouds. *Combust. Flame* **2025**, *273* paper 113932; https://doi.org/10.1016/j.combustflame.2024.113932.

[8] Huang, H.J.; Dong, H.S.; Zhang, M. Problems and Developments in Composition B Modification Research. *Energ. Mater.* **2001**, *9*(04): 183-186; https://doi.org/10.3969/j.issn.1006-9941.2001.04.011.

[9] Velicky, R.W.; Voigt, H.W.; Voreck, W.E. The Effect of Some Additives on the Closed Bomb Burning and Ignitability of RDX/TNT (60/40). *J. Energ. Mater.* **1985**, *3*(2): 129-148; https://doi.org/10.1080/07370658508012338.

[10] Hobbs, M.L.; Kaneshige, M.J.; Erikson, W.W.; Brown, J.A.; Anderson, M.U.; Todd, S.N.; Moore, D.G. Cookoff Modeling of a Melt Cast Explosive (Comp-B). *Combust. Flame* **2020**, *215*: 36-50; https://doi.org/10.1016/j.combustflame.2020.01.022.

[11] Sarangapani, R.; Ramavat, V.; Reddy, S.; Subramanian, P.; Sikder, A.K. Rheology Studies of NTO-TNT Based Melt-Cast Dispersions and Influence of Particle-Dispersant Interactions. *Powder Technol.* **2015**, *273*: 118-124; https://doi.org/10.1016/j.powtec.2014.12.013.

[12] Wang, Q.H. Overview of Carrier Explosive for Melt-cast Composite Explosive. *Chin. J. Explos. Propellants* **2011**, *34*(05): 25-28+42; https://doi.org/10.14077/j.issn.1007-7812.2011.05.010.

[13] Li, D.Y.; Cheng, Y.F.; Xu, J.W.; Wang, Z.H.; Zhao, C.X. Effects of Typical MH_2 (M= Ti, Mg, Zr) on the Detonation Energy Release Characteristics of Composite Charge Containing Al/PTFE Reactive Materials and RDX. *Vacuum* **2024**, *227* paper 113432; https://doi.org/10.1016/j.vacuum.2024.113432.
[14] Li, J.S.; Chen, J.J.; Hwang, C.C.; Lu, T.K.; Yeh, T.F. Study on Thermal Characteristics of TNT Based Melt-Cast Explosives. *Propellants Explos. Pyrotech.* **2019**, *44*(10): 1270-1281; https://doi.org/10.1002/prep.201900078.
[15] Zhai, X.; Zhang, Y.; Kang, G.; Chen, P. Simulation of the TNT-Based Melt-Cast Explosive Charging Process Using Hot Mandrel Assisted Solidification. *Comput. Struct.* **2025**, *315* paper 107780; https://doi.org/10.1016/j.compstruc.2025.107780.
[16] Wang, H.; Cheng, Y.F.; Zhu, S.J.; Li, Z.H.; Shen, Z.W. Effects of Content and Particle Size of TiH_2 Powders on the Energy Output Rules of RDX Composite Explosives. *Def. Technol.* **2024**, *32*: 297-308; https://doi.org/10.1016/j.dt.2023.05.002.
[17] Xiao, C.; Yu, Q.; Zheng, X.Y.; Zheng, B.; Guo, Y.; Luo, G.; Li, J. High-Performance and Insensitive DNTF-DFTNAN Eutectic: Binary Phase Diagram and Characterization. *Propellants Explos. Pyrotech.* **2022**, *47*(11) paper e202200166; https://doi.org/10.1002/prep.202200166.
[18] Zhao, F.Q.; Pei, C.; Hu, R.Z.; Luo, Y.; Zhang, Z.; Zhou, Y.; Yang, X.; Gao, Y.; Gao, S.; Shi, Q. Thermochemical Properties and Non-Isothermal Decomposition Reaction Kinetics of 3,4-Dinitrofurazanfuroxan (DNTF). *J. Hazard Mater.* **2004**, *113*(1-3): 67-71; https://doi.org/10.1016/J.JHAZMAT.2004.07.009.
[19] Wang, Q.H.; Zhang, Y.A.; Jin, D.Y. Energy and Castibility of DNTF Explosive. *Chin. J. Explos. Propellants* **2004**, *27*(04): 14-16; https://doi.org/10.3969/j.issn.1007-7812.2004.04.004.
[20] Zheng, W.; Wang, J.N. Review on 3,4-Bis-nitrofurazanfuroxan (DNTF). *Chin. J. Energ. Mater.* **2006**, *14*(06): 463-466; https://doi.org/10.3969/j.issn.1006-9941.2006.06.015.
[21] Yuan, J.; Huang, R.; Wang, J.; Xing, X.; Wang, J.; Han, T.; Yang, Q.; Yang, J. Experiment and Molecular Dynamic Simulation on Interactions between 3,4-Bis (3-nitrofurazan-4-yl) Furoxan (DNTF) and Some Low-Melting-Point Explosives. *Molecules* **2024**, *29*(16) paper 3757; https://doi.org/10.3390/molecules29163757.
[22] Chun, X.; You, R.; Lei, Y.; Baohui, Z.; Chuan, H.; Qing, M.; Jinshan, L. 3,4-Bis (3-nitrofurazan-4-yl) Furoxan (DNTF) and 4-Methoxy-1-methyl-3,5-dinitro-1H-pyrazole (DMDNP) Based Molten Carrier with High Energy and Low Sensitivity: Eutectic Design and Desensitization Effect. *Mater. Today Commun.* **2024**, *41* paper 110383; https://doi.org/10.1016/j.mtcomm.2024.110383.
[23] Wang, Q. Properties of DNTF-Based Melt-Cast Explosives. *Chin. J. Explos. Propellants* **2003**, *26*(3): 57-59; https://doi.org/10.3969/j.issn.1007-7812.2003.03.016.
[24] Shang, Y.; Yu, Z.H.; Huang, R.K.; Chen, S.L.; Liu, D.X.; Chen, X.X.; Zhang, W.X.; Chen, X.M. Metal-Free Hexagonal Perovskite High-Energetic Materials with $NH_3OH^+/NH_2NH_3^+$ as B-Site Cations. *Engineering* **2020**, *6*(9): 1013-1018; https://doi.org/10.1016/j.eng.2020.05.018.

[25] An, E.; Tan, Y.; Han, K.; Li, X.; Cao, X.; Tan, Y.; Deng, P. The Role of Fe Nanospheres in Energy Releasing of DAP-4. *Combust. Flame* **2023**, *257* paper 113014; https://doi.org/10.1016/j.combustflame.2023.113014.

[26] Shang, Y.; Huang, R.K.; Chen, S.L.; He, C.T.; Yu, Z.H.; Ye, Z.M.; Zhang, W.X.; Chen, X.M. Metal-Free Molecular Perovskite High-Energetic Materials. *Cryst. Growth Des.* **2020**, *20*(3): 1891-1897; https://doi.org/10.1021/acs.cgd.9b01592.

[27] Hu, L.; Du, Z.; Liu, Y.; Gong, S.; Guang, C.; Li, X.; Yang, Z.; Jia, Q.; Liang, K. Green Fabrication of Nanoscale Energetic Molecular Perovskite (H_2dabco)[$Na(ClO_4)_3$] with Reduced Mechanical Sensitivity. *Cent. Eur. J. Energ. Mater.* **2021**, *18*(3): 369-384; https://doi.org/10.22211/cejem/142572.

[28] Zhang, W.X.; Chen, S.L.; Shang, Y.; Yu, Z.H.; Chen, X.M. Molecular Perovskites as a New Platform for Designing Advanced Multi-Component Energetic Crystals. *Energ. Mater. Front.* **2020**, *1*(3-4): 123-135; https://doi.org/10.1016/j.enmf.2020.12.003.

[29] Liang, K.; Liu, Y.; Hu, L.; Liang, J.; Lv, T.; Wu, W.; Wang, Y.; Tu, Z.; Hu, S. Preparation and Combustion Performance of Molecular Perovskite Energetic Material DAP-4-Based Composite with Titanium Powder. *J. Therm. Anal. Calorim.* **2023**, *148*(22): 12739-12750; https://doi.org/10.1007/s10973-023-12572-9.

[30] Feng, X.J.; Zhang, K.; Shang, Y.; Pan, W. Thermal Decomposition Study of Perchlorate-Based Metal-Free Molecular Perovskite DAP-4 Mixed with Ammonium Perchlorate. *Case. Stud. Therm. Eng.* **2022**, *34* paper 102013; https://doi.org/10.1016/j.csite.2022.102013.

[31] Chen, S.L.; Yang, Z.R.; Wang, B.J.; Shang, Y.; Sun, L.Y.; He, C.T.; Zhou, H.L.; Zhang, W.X.; Chen, X.M. Molecular Perovskite High-Energetic Materials. *Sci China Mater.* **2018**, *61*(8): 1123-1128; https://doi.org/10.1007/s40843-017-9219-9.

[32] Hu, L.; Liu, Y.; He, D.; Yang, Y.; Gong, S.; Guang, C.; Deng, P.; Hu, S. Study of Molecular Perovskite (H_2dabco)[$NH_4(ClO_4)_3$]/Carbon Nanotubes Energetic Composite. *Cent. Eur. J. Energ. Mater.* **2022**, *19*(1): 91-105; https://doi.org/10.22211/cejem/147766.

[33] Yu, L.; Ren, H.; Guo, X.; Jiang, X.B.; Jiao, Q.J. A Novel ε-HNIW-based Insensitive High Explosive Incorporated with Reduced Graphene Oxide. *J. Therm. Anal. Calorim.* **2014**, *117*(03): 1187-1199; https://doi.org/10.1007/s10973-014-3928-7.

[34] Zhang, K.; Feng, B.; Wang, X.F. Thermal Decomposition Mechanism of DAP-4/TKX-50 Mixtures. *Chin. J. Energ. Mater.* **2022**, *30*(07): 673-680; https://doi.org/10.11943/CJEM2022064.

[35] Liu, Y.; Hu, L.; Gong, S.; Guang, C.; Li, L.; Hu, S.; Deng, P. Study of Ammonium Perchlorate-Based Molecular Perovskite (H_2DABCO)[$NH_4(ClO_4)_3$]/Graphene Energetic Composite with Insensitive Performance. *Cent. Eur. J. Energ. Mater.* **2020**, *17*(3): 451-469; https://doi.org/10.22211/cejem/127934.

Authorship contribution statement

Xi Zhang: conception, foundations, methods, performing the experimental part, performing the statistical analysis
Li Yan: performing the experimental part
Binfeng Sun: methods, performing the experimental part
Yibing Duan: performing the experimental part
Yu Qiu: performing the experimental part
Xiaoyu Shang: foundations
Fuxing Wang: foundations
Yang Liu: foundations
Li-shuang Hu: conception, foundations, methods, performing the statistical analysis

Submitted: August 26, 2025
Revised: March 27, 2026
First published online: March 31, 2026